

RADIATIVE TRANSFER IN AN ABSORBING AND ANISOTROPICALLY SCATTERING SLAB WITH A REFLECTING BOUNDARY*

G. SPIGA

Laboratorio Ingegneria Nucleare, Università di Bologna,
Via dei Colli, 16. I-40136 Bologna, Italy

F. SANTARELLI and C. STRAMIGIOLI

Istituto Impianti Chimici, Università di Bologna, Viale Risorgimento, 2. I-40136 Bologna, Italy

(Received 6 July 1979)

Abstract—Radiative transfer has been considered within a participating plane slab assuming the externally-applied radiation to impinge normally on one boundary of the slab while the other boundary is assumed to reflect in a diffuse way. The linearly anisotropic and the Rayleigh modes of scattering have been both considered. A rigorous solution is developed following a constructive procedure based on projectional methods: the resulting computational formulae have been numerically processed to obtain the distribution of the physically relevant variables for some significant situations.

NOMENCLATURE

a ,	optical half-thickness;
c ,	albedo;
E_n ,	n th exponential integral;
I ,	angular radiation intensity;
I_0 ,	total radiation intensity;
$q = I_1$,	net radiative flux;
q^+, q^- ,	forward, backward radiative flux.

Greek symbols

α ,	power entering at $\tau = -a$;
μ ,	cosine of the angle between the direction of the radiation intensity and the positive τ axis;
$\bar{\mu}_0$,	weighted average of the cosine of the scattering angle for the linearly anisotropic scattering case;
ρ ,	diffuse reflectivity of the boundary $\tau = a$;
τ ,	optical coordinate.

1. INTRODUCTION

THE PROBLEM of stationary radiative-heat transfer in an absorbing emitting and scattering plane-parallel medium has been investigated by many authors, and with different methods. Anisotropy of scattering and effects of diffuse and specular reflectivity of the bounding surfaces can be included in the analysis[1, 2].

Solving the resulting equations, even in simple, but significant problems, seems to be quite a difficult task; it has been accomplished up to now mostly by pure numerical schemes, or by resorting to drastic approxi-

mations[3-5]. Only in some recent approaches semi-analytical techniques have been proposed, in which the solution is carried out rigorously as far as possible, and numerical calculations are needed as a final step to determine the parameters entering the explicit expression of the physical quantities sought. It is worth mentioning Case's method[6], which requires rather heavy computations, and the integral transform method[7, 8], which, on the other hand, can be used only in highly idealized problems. A classical projection procedure[9] turns out to be very simple and effective in very general physical situations[10]: the procedure is constructive since we can build up an approximate solution as close as we wish to the exact solution. Numerical calculations are also straightforward.

Following the last approach above, and in the framework of the general theory presented in[1], we will study in this paper radiant energy transfer in an absorbing and anisotropically scattering slab subject to an external axisymmetric applied radiation at one of its surfaces, the other being diffusely reflecting. The physical interest of such a problem is well known[11, 12]. Temperature is supposed to be so low, that emission of medium and bounding surfaces can be neglected.

Temperature effects could, however, be taken into account without particular difficulties, as well as the effects of specular and/or diffuse reflectivity of the first boundary, or specular reflectivity of the second. The aim of the paper is to investigate how radiative transfer is affected by anisotropy of scattering (both linear and Rayleigh anisotropic scattering are considered), albedo and optical depth of the medium, and reflectivity of the boundary. Numerical results for the angular and the total radiation intensity and for the radiative heat flux are presented and discussed.

*Work supported by C.N.R., Roma. (Grant 78.02453.07/115.9364).

2. THEORY

In the physical situation considered above the linear integro-differential radiative-transfer equation is, in standard notation

$$\mu \frac{\partial I(\tau, \mu)}{\partial \tau} + I(\tau, \mu) = c \int_{-1}^1 K(\mu, \mu') I(\tau, \mu') d\mu', \quad (1)$$

with $-a \leq \tau \leq a$, $-1 \leq \mu \leq 1$, I being the angular-radiation intensity, and c the total albedo. For a finite order L of anisotropy, the scattering kernel $K(\mu, \mu')$ reads as

$$K(\mu, \mu') = \sum_{j=0}^L \frac{2j+1}{2} p_j P_j(\mu) P_j(\mu'), \quad (2)$$

where P_j denotes the j th Legendre polynomial [13], and p_j is the j th Legendre moment of the scattering-transfer function, which depends only on the angle θ_0 between the directions before and after collision. In particular $p_0 = 1$ and $p_1 = \bar{\mu}_0$, i.e. the weighted average of $\cos \theta_0$.

The Legendre moment of the unknown radiation intensity is defined as

$$I_j(\tau) = 2\pi \int_{-1}^1 I(\tau, \mu) P_j(\mu) d\mu \quad j = 0, 1, \dots, \quad (3)$$

with $I_0(\tau) =$ total incident intensity, and $I_1(\tau) = q(\tau) =$ net radiative heat flux. The unknown I is uniquely determined by equation (1) and the boundary conditions

$$I(-a, \mu) = \frac{\alpha}{2\pi} h(\mu),$$

$$I(a, -\mu) = \rho g(\mu) \int_0^1 \mu' I(a, \mu') d\mu', \quad \mu > 0 \quad (4)$$

α being the total power entering the medium through the plane $\tau = -a$, $h(\mu)$ its angular distribution, and $\rho \leq 1$ the diffuse reflectivity of the other surface $\tau = a$. The function $g(\mu)$ accounts for the angular distribution of reflected radiation.

Formal solution of equation (1) upon conditions (4) yields, for $\mu > 0$

$$I(\tau, \mu) = \frac{c}{4\pi} \sum_{j=0}^L (2j+1) p_j \frac{P_j(\mu)}{\mu} \times \int_{-a}^{\tau} e^{-(\tau-\tau')/\mu} I_j(\tau') d\tau' + \frac{\alpha}{2\pi} e^{-(a+\tau)/\mu} h(\mu), \quad (5a)$$

$$I(\tau, -\mu) = \frac{c}{4\pi} \sum_{j=0}^L (2j+1) (-1)^j p_j \frac{P_j(\mu)}{\mu} \times \int_{\tau}^a e^{(\tau-\tau')/\mu} I_j(\tau') d\tau' + \rho e^{-(a-\tau)/\mu} g(\mu) \times \int_0^1 \mu' I(a, \mu') d\mu'. \quad (5b)$$

$I(\tau, \mu)$ is thus completely given in terms of the $L+2$ functions I_0, I_1, \dots, I_L and $I(a, \mu)$. Such functions can be found operating on equations (5) themselves. $I(a, \mu)$ is

in fact reproduced by equation (5a), specialized for $\tau = a$, and $I_j(\tau)$ by taking Legendre moments of $I(\tau, \mu)$ as expressed by equation (5). Eliminating then $I(a, \mu)$ in the resulting equations, one gets

$$I_i(\tau) = c \sum_{j=0}^L \frac{2j+1}{2} p_j \int_{-a}^a H_{ij}(\tau, \tau') \times I_j(\tau') d\tau' + F_i(\tau), \quad i = 0, 1, \dots, \quad (6)$$

where

$$H_{ij}(\tau, \tau') = \text{sgn}(\tau - \tau')^{i+j} K_{ij}(|\tau - \tau'|) + \frac{1}{2} \rho (-1)^i G_i(\tau) G_j(\tau'), \quad (7a)$$

$$F_i(\tau) = \alpha \int_0^1 P_i(\mu) h(\mu) e^{-(a+\tau)/\mu} d\mu + (-1)^i \rho \alpha G_i(\tau) \int_0^1 \mu e^{-(2a)/\mu} h(\mu) d\mu, \quad (7b)$$

with $\text{sgn } x = |x|/x$, and

$$K_{ij}(x) = \int_0^1 \frac{e^{-x/\mu}}{\mu} P_i(\mu) P_j(\mu) d\mu; \quad x > 0, \quad (8a)$$

$$G_i(\tau) = \int_0^1 P_i(\mu) g(\mu) e^{-(a-\tau)/\mu} d\mu. \quad (8b)$$

All K_{ij} functions can be simply expressed in terms of exponential integrals [13]

$$E_n(x) = \int_0^1 \mu^{n-2} e^{-x/\mu} d\mu; \quad (9)$$

the first few are listed in Appendix 1.

When the index i in equation (6) runs from 0 to L , we have a linear system of $L+1$ integral equations for the $L+1$ unknowns I_0, I_1, \dots, I_L , in which all effects of reflection are incorporated exactly in the kernels and known terms. The system can be solved easily and rigorously by a projection procedure already adopted in [14] for a problem of neutron transport, i.e. by expanding all moments as

$$I_j(\tau) = \sum_{n=0}^N \left(\frac{2n+1}{2a} \right)^{1/2} \eta_n^j P_n \left(\frac{\tau}{a} \right) \quad j = 0, 1, \dots, L, \quad (10)$$

where

$$\eta_n^j = \left(\frac{2n+1}{2a} \right)^{1/2} \int_{-a}^a P_n \left(\frac{\tau}{a} \right) I_j(\tau) d\tau. \quad (11)$$

Equation (10) is then used in equation (6), which is finally multiplied through by $[(2m+1)/2a]^{1/2} P_m(\tau/a)$, $m = 0, 1, \dots, N$, and integrated from $-a$ to $+a$, to get a linear algebraic system of $(L+1)(N+1)$ equations for the $(L+1)(N+1)$ unknown coefficients η_n^j . This constructive procedure yields a sequence of approximate solutions, whose convergence to the exact solution when $N \rightarrow +\infty$ is guaranteed *a priori* [1, 10, 14]; the less conservative the medium, the faster the convergence rate, which however has always been extremely satisfactory in all considered cases, so that

only rather small values of N have been required. Once the I_j s, $j=0,1,\dots,L$, are known up to the desired degree of accuracy, the angular-radiation intensity follows from equations (5) and its higher moments I_{L+1}, I_{L+2}, \dots from equation (6). Also the partial radiative heat fluxes q^+ and q^- , with $q^+(\tau) - q^-(\tau) = q(\tau)$, can be explicitly evaluated as

$$q^+(\tau) = 2\pi \int_0^1 \mu I(\tau, \mu) d\mu, \\ q^-(\tau) = 2\pi \int_0^1 \mu I(\tau, -\mu) d\mu. \quad (12)$$

3. APPLICATIONS

We will consider two examples with different order of anisotropy. In both cases the externally applied radiation is normalized to $\alpha = 1$, and enters the medium normally to the first bounding surface, and radiation reflected from the second boundary is isotropic. In symbols

$$h(\mu) = \delta(\mu - 1), \quad g(\mu) = 2. \quad (13)$$

The functions G_i , equation (8b), and F_i , equation (7b), can be thus evaluated explicitly. The first few are reported in Appendix 1.

3.1. Linearly anisotropic scattering

We take $L=1$ in equation (2), with $p_1 = \bar{\mu}_0$ ranging from $-\frac{1}{3}$ to $+\frac{1}{3}$ since $K(\mu, \mu')$ must always be positive. A positive (negative) $\bar{\mu}_0$ means forward (backward) scattering, $\bar{\mu}_0 = 0$ corresponds to isotropic scattering. The angular radiation intensity is given by

$$I(\tau, \mu) = \frac{c}{4\pi} \frac{1}{\mu} \int_{-a}^{\tau} e^{-(\tau-\tau')/\mu} I_0(\tau') d\tau' \\ + \frac{c}{4\pi} 3\bar{\mu}_0 \int_{-a}^{\tau} e^{-(\tau-\tau')/\mu} I_1(\tau') d\tau' \\ + \frac{1}{2\pi} e^{-(a+\tau)} \delta(\mu - 1), \quad (14a)$$

$$I(\tau, -\mu) = \frac{c}{4\pi} \frac{1}{\mu} \int_{\tau}^a e^{(\tau-\tau')/\mu} I_0(\tau') d\tau' \\ + 2\rho \frac{c}{4\pi} e^{-(a-\tau)/\mu} \int_{-a}^a E_2(a-\tau') I_0(\tau') d\tau' \\ - \frac{c}{4\pi} 3\bar{\mu}_0 \int_{\tau}^a e^{(\tau-\tau')/\mu} I_1(\tau') d\tau' \\ + 2\rho \frac{c}{4\pi} 3\bar{\mu}_0 e^{-(a-\tau)/\mu} \int_{-a}^a E_3(a-\tau') \\ \times I_1(\tau') d\tau' + 2\rho \frac{1}{2\pi} e^{-2a} e^{-(a-\tau)/\mu}, \quad (14b)$$

in terms of its first two moments I_0 and I_1 only, which are solution to the system of two coupled linear integral equations

$$I_0(\tau) = \frac{1}{2}c \int_{-a}^a H_{00}(\tau, \tau') I_0(\tau') d\tau'$$

$$+ \frac{3}{2}\bar{\mu}_0 c \int_{-a}^a H_{01}(\tau, \tau') I_1(\tau') d\tau' + F_0(\tau), \quad (15a)$$

$$I_1(\tau) = \frac{1}{2}c \int_{-a}^a H_{10}(\tau, \tau') I_0(\tau') d\tau' \\ + \frac{3}{2}\bar{\mu}_0 c \int_{-a}^a H_{11}(\tau, \tau') I_1(\tau') d\tau' + F_1(\tau), \quad (15b)$$

whose kernels are listed in Appendix 1. We have now to expand I_0 and I_1 according to equation (10), and to use such expansions in the RHS of equations (15). The result reads as

$$I_i(\tau) = e^{-(a-\tau)} + 2(-1)^i e^{-2a} \rho E_{2+i}(a-\tau) \\ + \sum_{n=0}^N \left(\frac{2n+1}{2a} \right)^{1/2} \eta_n^0 \left[\frac{1}{2} c U_n^i(\tau) \right. \\ \left. + (-1)^i c \rho D_n^0 E_{2+i}(a-\tau) \right] \\ + \sum_{n=0}^N \left(\frac{2n+1}{2a} \right)^{1/2} \eta_n^1 \left[\frac{3}{2} \bar{\mu}_0 c U_n^{1+i}(\tau) \right. \\ \left. + (-1)^i 3\bar{\mu}_0 c \rho D_n^1 E_{2+i}(a-\tau) \right] \quad i = 0, 1, \quad (16)$$

where the known functions $U_n^s(\tau)$ and constant D_n^s are given by

$$U_n^s(\tau) = \int_{-a}^a \text{sgn}(\tau - \tau')^s E_{1+s}(|\tau - \tau'|) P_n \left(\frac{\tau'}{a} \right) d\tau' \quad (17)$$

and

$$D_n^s = \int_{-a}^a E_{2+s}(a-\tau) P_n \left(\frac{\tau}{a} \right) d\tau, \quad (18)$$

respectively. The unknown expansion coefficients η_n^i can in turn be obtained from the linear algebraic system

$$\eta_m^i = F_m^i + \sum_{j=0}^1 \sum_{n=0}^N \frac{[(2m+1)(2n+1)]^{1/2}}{2a} G_{mn}^{ij} \eta_n^j, \quad (19)$$

$$m = 0, 1, \dots, N; \quad i = 0, 1$$

with matrix elements

$$G_{mn}^{ij} = \frac{1}{2}c(3\bar{\mu}_0)^j [C_{mn}^{i+j} + (-1)^i 2\rho D_m^i D_n^j], \quad (20)$$

where

$$C_{mn}^s = \int_{-a}^a P_m \left(\frac{\tau}{a} \right) d\tau \int_{-a}^a \text{sgn}(\tau - \tau')^s \\ \times E_{1+s}(|\tau - \tau'|) P_n \left(\frac{\tau'}{a} \right) d\tau', \quad (21)$$

and inhomogeneous terms

$$F_n^s = \left(\frac{2n+1}{2a} \right)^{1/2} [E_n + (-1)^s 2\rho e^{-2a} D_n^s] \quad (22)$$

where

$$E_n = (-1)^n \int_{-a}^a e^{-(a-\tau)} P_n \left(\frac{\tau}{a} \right) d\tau. \quad (23)$$

All integrals in equations (17), (18), (21) and (23) can be evaluated analytically, as shown in Appendix 2. Once the $2N + 2$ coefficients η_n^0 and η_n^1 are found from the algebraic system, equation (19), equations (16) yield, more accurately than (10), $I_0(\tau)$ and $I_1(\tau)$, and moreover we get

$$I(\tau, \mu) = \frac{c}{4\pi} \sum_{n=0}^N \left(\frac{2n+1}{2a}\right)^{1/2} \eta_n^0 W_n(\tau, \mu) + \frac{c}{4\pi} 3\bar{\mu}_0 \sum_{n=0}^N \left(\frac{2n+1}{2a}\right)^{1/2} \eta_n^1 \mu W_n(\tau, \mu) + \frac{1}{2\pi} e^{-(a+\tau)} \delta(\mu - 1), \tag{24a}$$

$$I(\tau, -\mu) = 2\rho \frac{1}{2\pi} e^{-2a} e^{-(a-\tau)\mu} + \frac{c}{4\pi} \sum_{n=0}^N \left(\frac{2n+1}{2a}\right)^{1/2} \eta_n^0 [(-1)^n W_n(-\tau, \mu) + 2\rho D_n^0 e^{-(a-\tau)/\mu}] - \frac{c}{4\pi} 3\bar{\mu}_0 \sum_{n=0}^N \left(\frac{2n+1}{2a}\right)^{1/2} \eta_n^1 [(-1)^n \mu \times W(-\tau, \mu) - 2\rho D_n^1 e^{-(a-\tau)/\mu}], \tag{24b}$$

with

$$W_n(\tau, \mu) = \frac{1}{\mu} \int_{-a}^{\tau} e^{-(\tau-\tau')/\mu} P_n\left(\frac{\tau'}{a}\right) d\tau', \tag{25}$$

and

$$q^+(\tau) = \frac{c}{2} \sum_{n=0}^N \left(\frac{2n+1}{2a}\right)^{1/2} \eta_n^0 G_n^0(\tau) + \frac{c}{2} 3\bar{\mu}_0 \times \sum_{n=0}^N \left(\frac{2n+1}{2a}\right)^{1/2} \eta_n^1 G_n^1(\tau) + e^{-(a+\tau)}, \tag{26a}$$

$$q^-(\tau) = 2\rho e^{-2a} E_3(a - \tau) + \frac{c}{2} \sum_{n=0}^N \left(\frac{2n+1}{2a}\right)^{1/2} \eta_n^0 [(-1)^n G_n^0(-\tau) + 2\rho D_n^0 E_3(a - \tau)] - \frac{c}{2} 3\bar{\mu}_0 \sum_{n=0}^N \left(\frac{2n+1}{2a}\right)^{1/2} \eta_n^1 \times [(-1)^n G_n^1(-\tau) - 2\rho D_n^1 E_3(a - \tau)], \tag{26b}$$

with

$$G_n^s(\tau) = \int_{-a}^{\tau} E_{2+s}(\tau - \tau') P_n\left(\frac{\tau'}{a}\right) d\tau'. \tag{27}$$

The functions W_n and G_n^s are also explicitly given in Appendix 2. It can be noticed that

$$I(\tau, 0) = \frac{c}{4\pi} I_0(\tau), \quad \tau \neq \pm a, \quad q^+(-a) = 1, \quad q^-(a) = \rho q^+(a). \tag{28}$$

3.2. Rayleigh scattering

We must take now $L = 2$ in equation (2), and set

$p_1 = 0$ and $p_2 = (1/10)$. The angular radiation intensity is given by

$$I(\tau, \mu) = \frac{c}{4\pi} \frac{1}{\mu} \int_{-a}^{\tau} e^{-(\tau-\tau')/\mu} I_0(\tau') d\tau' + \frac{c}{4\pi} \frac{1}{2} \frac{P_2(\mu)}{\mu} \int_{-a}^{\tau} e^{-(\tau-\tau')/\mu} I_2(\tau') d\tau' + \frac{1}{2\pi} e^{-(a+\tau)} \delta(\mu - 1), \tag{29a}$$

$$I(\tau, -\mu) = 2\rho \frac{1}{2\pi} e^{-2a} e^{-(a-\tau)/\mu} + \frac{c}{4\pi} \frac{1}{\mu} \int_{\tau}^a e^{(\tau-\tau')/\mu} I_0(\tau') d\tau' + 2\rho \frac{c}{4\pi} e^{-(a-\tau)/\mu} \int_{-a}^a E_2(a - \tau') I_0(\tau') d\tau' + \frac{c}{4\pi} \frac{1}{2} \frac{P_2(\mu)}{\mu} \int_{\tau}^a e^{(\tau-\tau')/\mu} I_2(\tau') d\tau' + \rho \frac{c}{4\pi} e^{-(a-\tau)/\mu} \frac{1}{2} \int_{-a}^a [3E_4(a - \tau') - E_2(a - \tau')] I_2(\tau') d\tau', \tag{29b}$$

and involves the moments I_0 and I_2 only. They are solutions to the system of two linear integral equations

$$I_0(\tau) = \frac{1}{2} c \int_{-a}^a H_{00}(\tau, \tau') I_0(\tau') d\tau' + \frac{1}{4} c \int_{-a}^a H_{02}(\tau, \tau') I_2(\tau') d\tau' + F_0(\tau), \tag{30a}$$

$$I_2(\tau) = \frac{1}{2} c \int_{-a}^a H_{20}(\tau, \tau') I_0(\tau') d\tau' + \frac{1}{4} c \int_{-a}^a H_{22}(\tau, \tau') I_2(\tau') d\tau' + F_2(\tau), \tag{30b}$$

whose kernels are reported in Appendix 1. Expanding I_0 and I_2 in the RHS of equations (30) according to equations (10), and following the same procedure previously proposed, yields for the expansion coefficients η_m^0 and η_m^2 the linear algebraic system of order $2N + 2$

$$\eta_m^{2i} = F_m^{2i} + \sum_{j=0}^1 \sum_{n=0}^N \frac{[(2m+1)(2n+1)]^{1/2}}{2a} G_{m,n}^{2i,2j} \eta_n^{2j} \tag{31}$$

$$m = 0, 1, \dots, N; \quad i = 0, 1,$$

where

$$F_m^2 = \left(\frac{2m+1}{2a}\right)^{1/2} [E_m + \rho e^{-2a} (3D_m^2 - D_m^0)], \tag{32}$$

and

$$G_{mn}^{02} = \frac{1}{4} c \left(\frac{3}{2} C_{mn}^2 - \frac{1}{2} C_{mn}^0\right) + \frac{1}{4} c \rho D_m^0 (3D_n^2 - D_n^0), \tag{33a}$$

$$G_{mn}^{20} = \frac{1}{2} c \left(\frac{3}{2} C_{mn}^2 - \frac{1}{2} C_{mn}^0\right) + \frac{1}{2} c \rho (3D_m^2 - D_m^0) D_n^0, \tag{33b}$$

$$G_{mn}^{22} = \frac{1}{4}c\left(\frac{3}{4}C_{mn}^4 - \frac{3}{2}C_{mn}^2 + \frac{1}{4}C_{mn}^0\right) + \frac{1}{8}c\rho(3D_m^2 - D_m^0)(3D_n^2 - D_n^0). \quad (33c)$$

All quantities of physical interest can then be expressed in terms of η_n^0 and η_n^2 , solution to equation (31). In fact we get

$$I(\tau, \mu) = \frac{c}{4\pi} \sum_{n=0}^N \left(\frac{2n+1}{2a}\right)^{1/2} \eta_n^0 W_n(\tau, \mu) + \frac{c}{4\pi} \sum_{n=0}^N \left(\frac{2n+1}{2a}\right)^{1/2} \eta_n^2 P_2(\mu) W_n(\tau, \mu) + \frac{1}{2\pi} \exp(-(a+\tau))\delta(\mu-1), \quad (34a)$$

$$I(\tau, -\mu) = 2\rho \frac{1}{2\pi} e^{-2a} e^{-(a-\tau)/\mu} + \frac{c}{4\pi} \sum_{n=0}^N \left(\frac{2n+1}{2a}\right)^{1/2} \eta_n^0 \left[(-1)^n W_n(-\tau, \mu) + 2\rho D_n^0 \exp\left(-\frac{a-\tau}{\mu}\right)\right] + \frac{c}{4\pi} \frac{1}{2} \times \sum_{n=0}^N \left(\frac{2n+1}{2a}\right)^{1/2} \eta_n^2 \left[(-1)^n P_2(\mu) W_n(-\tau, \mu) + \rho(3D_n^2 - D_n^0) \exp\left(-\frac{a-\tau}{\mu}\right)\right], \quad (34b)$$

for the angular intensity,

$$I_0(\tau) = \exp(-(a+\tau)) + 2\rho \exp(-2a) E_2(a-\tau) + \sum_{n=0}^N \left(\frac{2n+1}{2a}\right)^{1/2} \eta_n^0 \left[\frac{1}{2}c U_n^0(\tau) + c\rho D_n^0 E_2(a-\tau)\right] + \sum_{n=0}^N \left(\frac{2n+1}{2a}\right)^{1/2} \eta_n^2 \left[\frac{3}{4}c \left[\frac{3}{2} U_n^2(\tau) - \frac{1}{2} U_n^0(\tau)\right] + \frac{1}{4}c\rho(3D_n^2 - D_n^0) E_2(a-\tau)\right], \quad (35)$$

for the total incident intensity,

$$q^+(\tau) = e^{-(a+\tau)} + \frac{c}{2} \sum_{n=0}^N \left(\frac{2n+1}{2a}\right)^{1/2} \eta_n^0 G_n^0(\tau) + \frac{c}{2} \frac{1}{2} \sum_{n=0}^N \left(\frac{2n+1}{2a}\right)^{1/2} \eta_n^2 \left[\frac{3}{2} G_n^2(\tau) - \frac{1}{2} G_n^0(\tau)\right], \quad (36a)$$

$$q^-(\tau) = 2\rho e^{-2a} E_3(a-\tau) + \frac{c}{2} \sum_{n=0}^N \left(\frac{2n+1}{2a}\right)^{1/2} \eta_n^0 \left[(-1)^n G_n^0(-\tau) + 2\rho D_n^0 E_3(a-\tau)\right] + \frac{c}{2} \frac{1}{2} \sum_{n=0}^N \left(\frac{2n+1}{2a}\right)^{1/2} \eta_n^2 \left[\frac{3}{2} (-1)^n G_n^2(-\tau) - \frac{1}{2} (-1)^n G_n^0(-\tau) + \rho(3D_n^2 - D_n^0) E_3(a-\tau)\right], \quad (36b)$$

for the partial radiative heat fluxes. $I_1(\tau)$ can be evaluated as $I_1(\tau) = q^+(\tau) - q^-(\tau)$. Again it is worth

noticing that

$$I(\tau, 0) = \frac{c}{4\pi} [I_0(\tau) - \frac{1}{4}I_2(\tau)], \quad \tau \neq \pm a, \quad (37)$$

$$q^+(-a) = 1, \quad q^-(a) = \rho q^+(a).$$

4. NUMERICAL RESULTS AND COMMENTS

Values of a in the range 0.1–2.5 have been considered for both the anisotropic scattering modes assumed and for $\rho = 0, 0.5, 1.0$.

4.1. Linearly anisotropic scattering

Only the case $c = 0.9$ will be reported, as significant of situations where scattering is the prevailing mechanism through which radiation interacts with the material continuum and where, therefore, the effects of the scattering mode are magnified. For each value of a the cases $\bar{\mu}_0 = \frac{1}{3}$ (forward scattering), $\bar{\mu}_0 = 0$ (isotropic scattering) and $\bar{\mu}_0 = -\frac{1}{3}$ (backward scattering) have been considered.

The distributions of I_0 which result for the situations examined are given in Fig. 1 while the distributions of q are given in Fig. 2. The effects due to the forwardness of the scattering can be clearly grasped in the case of a transparent boundary ($\rho = 0$) at $\tau = a$ (Figs. 1-A and 2-A), if one reminds that I_0 is proportional, through $(1-c)$, to the local volumetric rate of energy absorption. Since forward (backward) scattering increases (decreases) the probability for a photon to proceed within the slab further than in the isotropic scattering case without experiencing absorption, it is then obvious that, close to the boundary $\tau = -a$, the curve for $\bar{\mu}_0 = \frac{1}{3}$ ($-\frac{1}{3}$) is lower (higher) than the isotropic scattering curve, while it is higher (lower) far enough from this boundary. The resulting trends and particularly the maximum which appears for the highest values of a are due to the boundary condition assumed at $\tau = -a$ coupled to the high value of c considered (for $c = 0.2$, the curves, not given here, exhibit the usual exponential-like decreasing trend and the maximum does not appear).

As far as the net radiative flux q is concerned, being $q = q^+ - q^-$, no crossing results between the q curves for $\bar{\mu}_0 > 0$, $\bar{\mu}_0 = 0$, $\bar{\mu}_0 < 0$ since, assuming the $\bar{\mu}_0 = 0$ case as the reference one, forward (backward) scattering causes a larger (smaller) q^+ and a smaller (larger) q^- to occur and therefore a higher (lower) curve results for q . It must be furthermore noted that the transmissivity of the slab is higher (lower) for $\bar{\mu}_0 > 0$ (< 0), since the corresponding mode of scattering causes a larger (smaller) number of photons to escape from the slab through the boundary $\tau = a$.

When the boundary $\tau = a$ is assumed to reflect in a diffuse way the shape and the relative departure of the curves at different $\bar{\mu}_0$ are changed according to the values of ρ and a considered. For $a = 0.1$ the difference between the I_0 curves at different values of $\bar{\mu}_0$ decreases when ρ increases and practically disappears when $\rho = 1$. The optically thin limit is approached for this

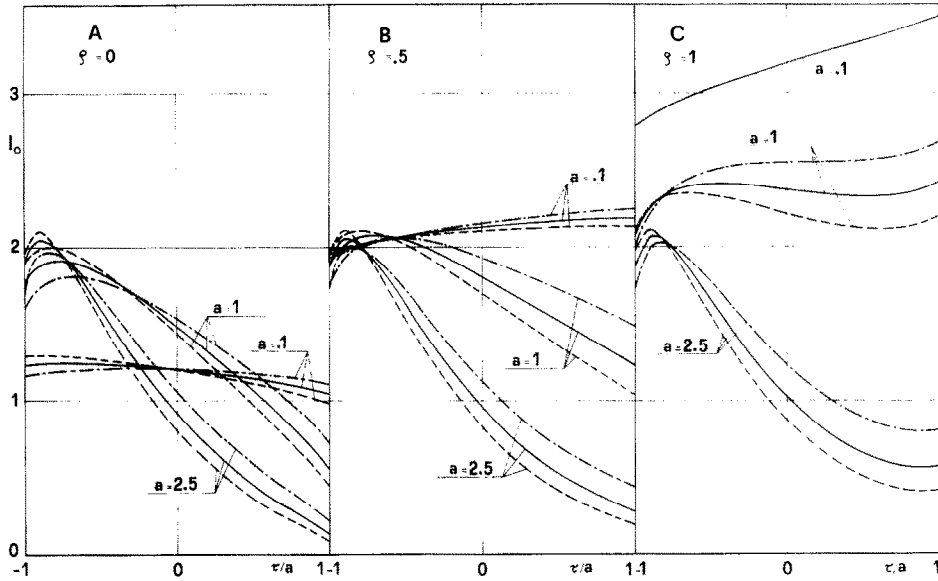


FIG. 1. Linearly anisotropic scattering: the total radiation intensity $I_0(\tau)$ as a function of τ/a for $c = 0.9$. (--- $\bar{\mu}_0 = -1/3$, — $\bar{\mu}_0 = 0$, - - - $\bar{\mu}_0 = 1/3$).

value of a and when $\rho = 1$ the flux of the reflected photons which re-enter into the slab is of same order of magnitude as the flux entering through the boundary $\tau = -a$: a sort of compensation therefore occurs and a situation typical of isotropic scattering, with no prevailing directional effects, occurs whatever the value of $\bar{\mu}_0$. The increasing trend which results for both the values of ρ considered is obviously due to the reflecting boundary which allows only a fraction $(1 - \rho)$ of the photons reaching the boundary to 'escape through it' from the slab.

For $a = 1.0, 2.5$, i.e. for intermediate-high values of

the optical thickness, the curves at different values of $\bar{\mu}_0$ maintain their own individuality since absorption is no longer negligible and therefore the flux of photons which re-enter into the slab at $\tau = a$ is largely lower than the one entering at $\tau = -a$: the mechanism working in optically thinner case is not effective any more.

As a result of the relevance of absorption, reflection significantly affects radiative transfer in the region close to the reflecting boundary for a depth depending on the value of a . This is apparent from Figs. 1-B, C where the most evident feature of the I_0 distributions is

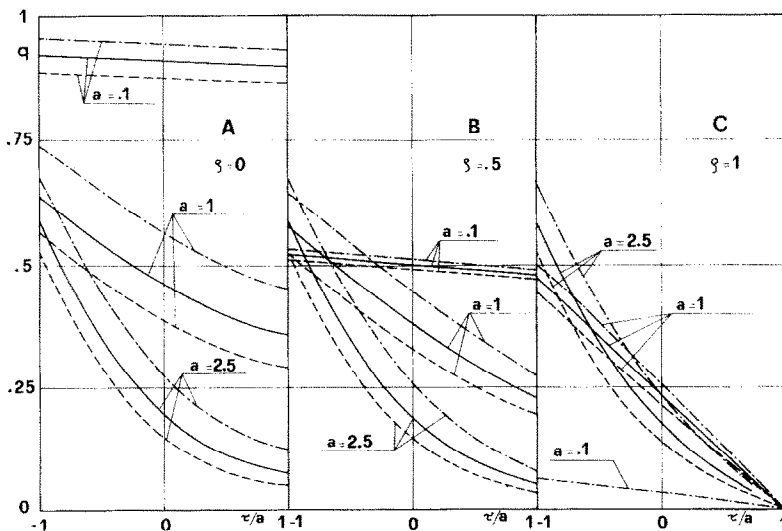


FIG. 2. Linearly anisotropic scattering: the net radiative flux $q(\tau)$ as a function of τ/a for $c = 0.9$. (--- $\bar{\mu}_0 = -1/3$, — $\bar{\mu}_0 = 0$, - - - $\bar{\mu}_0 = 1/3$).

a substantially uniform behavior for $a = 1.0$, while for $a = 2.5$ a marked rising of the curves results in the proximity of the reflecting boundary, no significant change occurring close to the boundary $\tau = -a$.

It must be furthermore noted that the influence of the reflecting boundary is slightly more pronounced in the forward scattering case since this scattering mode makes more photons available for reflection at $\tau = a$.

The influence of the reflecting boundary on the q distribution (Figs. 2-B, C) can easily be interpreted on the basis of all the arguments previously used: since reflection mainly affects the value of q^- , when ρ is increased the q curves are drastically lowered for low values of a , while they are noticeably reduced only close to the reflecting boundary when a higher optical thickness is considered. The angular distribution of $I(\tau, \mu)$ is given in Figs. 3-5 for some significant situations. The resulting curves can be interpreted straightforwardly and no specific comment will be deserved to them. It must only be noted that, owing to the boundary conditions assumed at $\tau = -a$, for any τ , it is $I(\tau, 1) = \infty$, as it results from equation (24a) too.

4.2. Rayleigh scattering

Two values of c (0.2, 0.9) have been considered as significant of situations where the prevailing interaction of the radiation with the material continuum is due to absorption and scattering respectively. The resulting I_0 and q distribution are given in Figs. 6 and 7.

No substantial difference arises with respect to the linearly anisotropic case and the influence of a reflecting boundary on the radiative transfer can be explained on the basis of the same arguments used there. Since the relevance of the absorption process plays a significant role in setting the resulting effects, the same trends result when a is increased for any given c or when c is decreased for any given a .

It must be furthermore noted that when the resulting values of I_0 are multiplied by $(1 - c)$ the curves giving the distribution of the local volumetric rate of energy absorption are lower for $c = 0.9$ than for $c = 0.2$, as physically due.

The angular distribution of $I(\tau, \mu)$ is given in Fig. 8 for $a = 1$ and $c = 0.9$ at different values of ρ and τ .

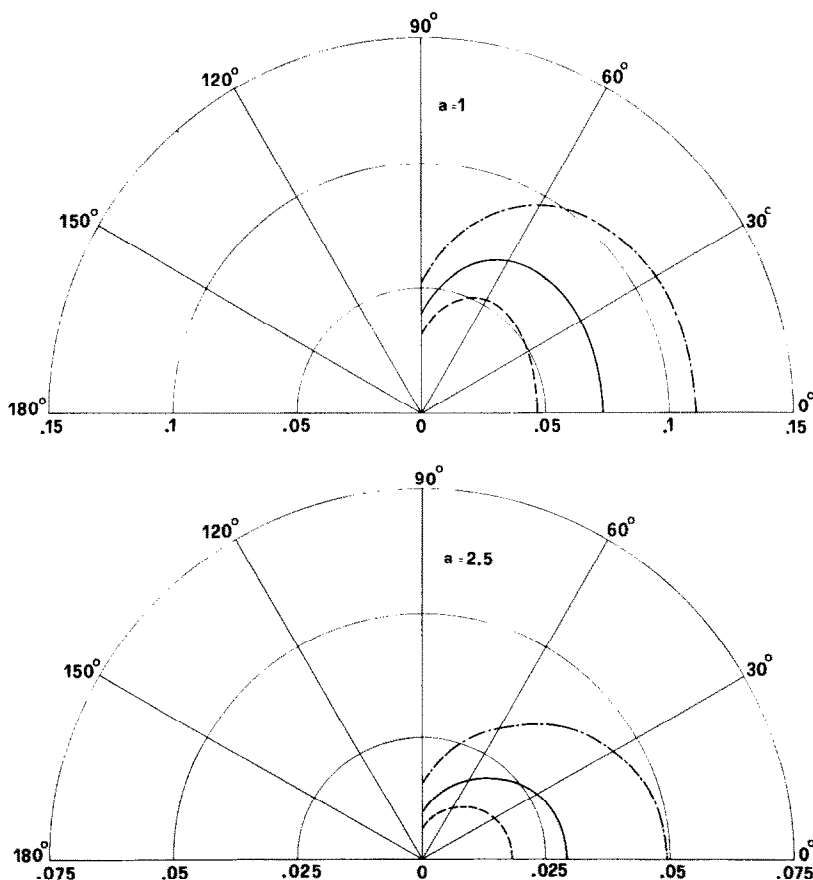


FIG. 3. Linearly anisotropic scattering: the angular distribution of the radiation intensity $I(\tau, \mu)$ at $\tau = a$ for $c = 0.9, \rho = 0$. (--- $\bar{\mu}_0 = -1/3$, — $\bar{\mu}_0 = 0$, - · - $\bar{\mu}_0 = 1/3$).

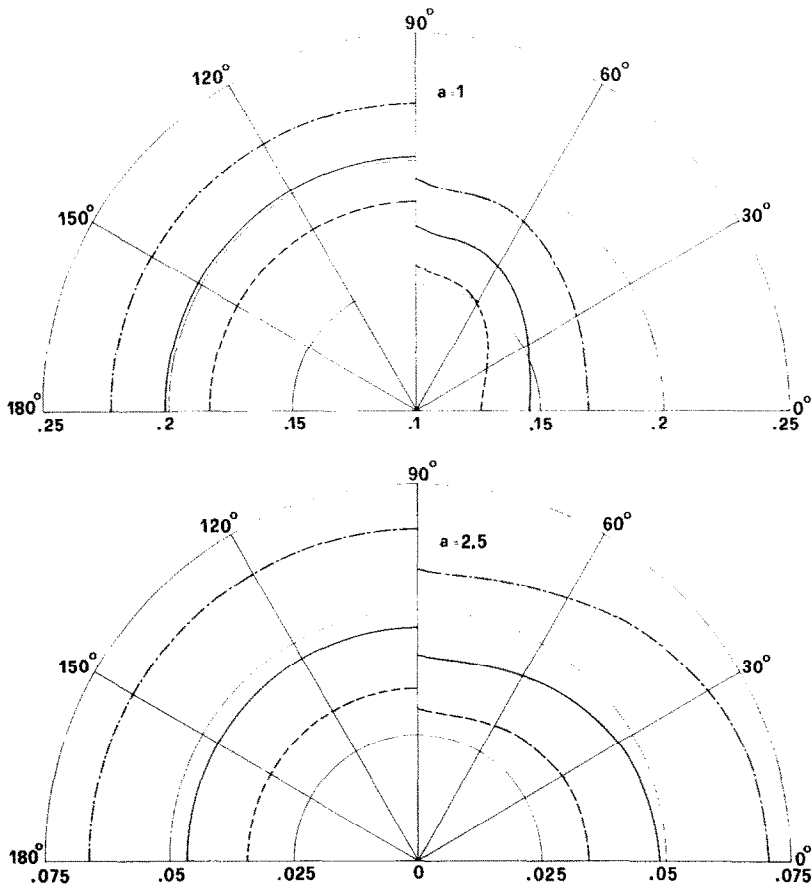


FIG. 4. Linearly anisotropic scattering: the angular distribution of the radiation intensity $I(\tau, \mu)$ at $\tau = a$ for $c = 0.9, \rho = 1$. (--- $\bar{\mu}_0 = -1/3$, — $\bar{\mu}_0 = 0$, - · - $\bar{\mu}_0 = 1/3$).

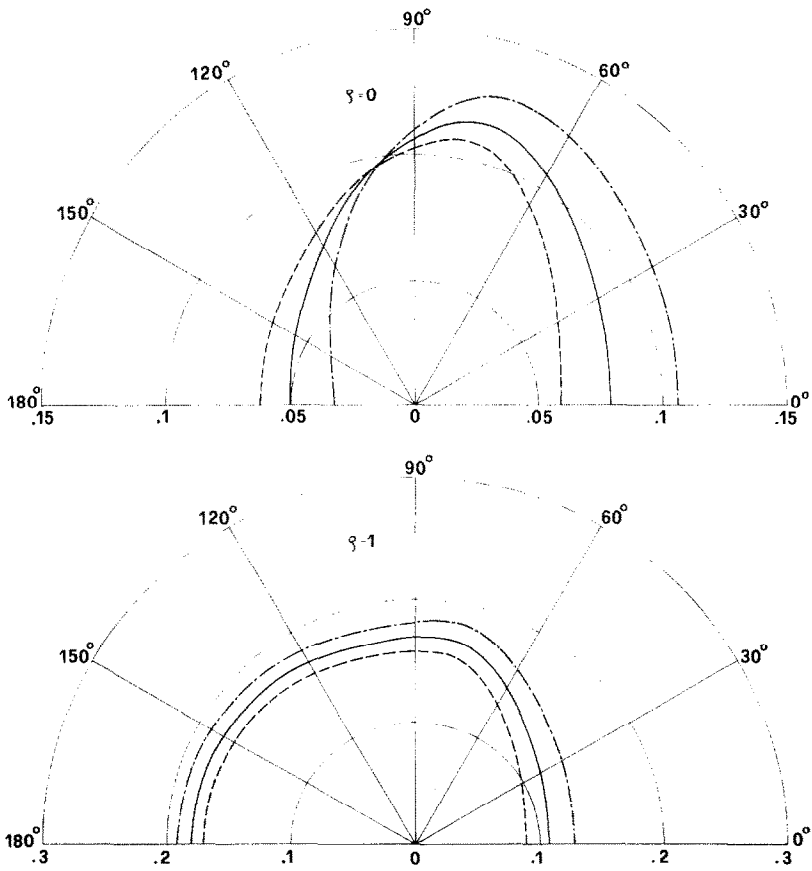


FIG. 5. Linearly anisotropic scattering: the angular distribution of the radiation intensity $I(\tau, \mu)$ at $\tau = 0$ for $a = 1, c = 0.9$. (--- $\bar{\mu}_0 = -1/3$, — $\bar{\mu}_0 = 0$, - · - $\bar{\mu}_0 = 1/3$).

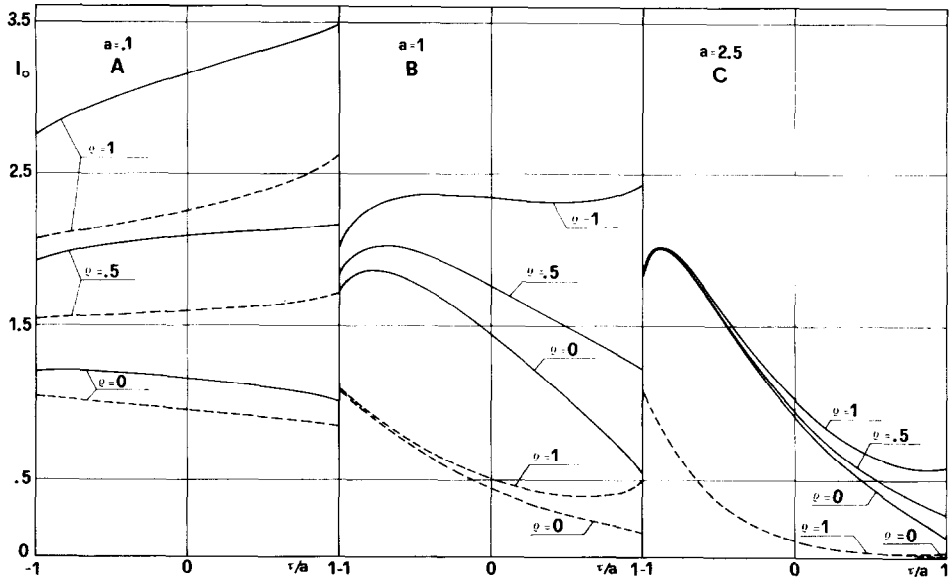


FIG. 6. Rayleigh scattering: the total radiation intensity $I_0(\tau)$ as a function of τ/a . (--- $c = 0.2$, — $c = 0.9$).

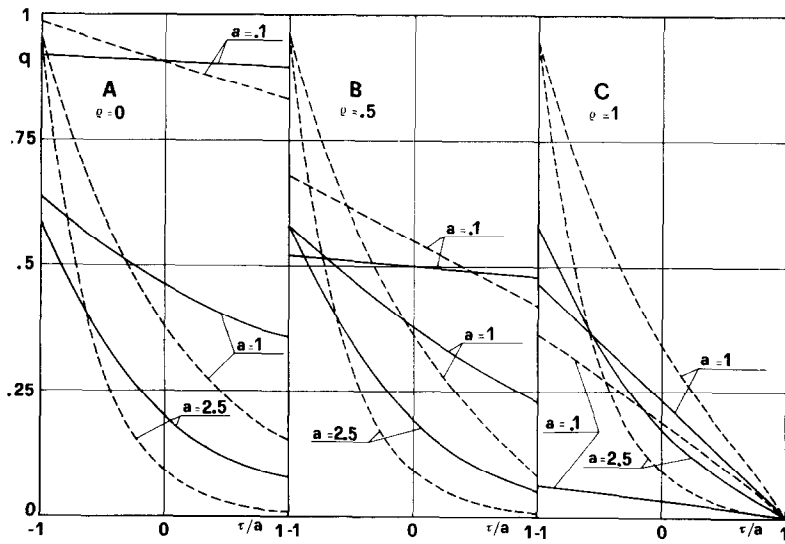


FIG. 7. Rayleigh scattering: the net radiative flux $q(\tau)$ as a function of τ/a . (--- $c = 0.2$, — $c = 0.9$).

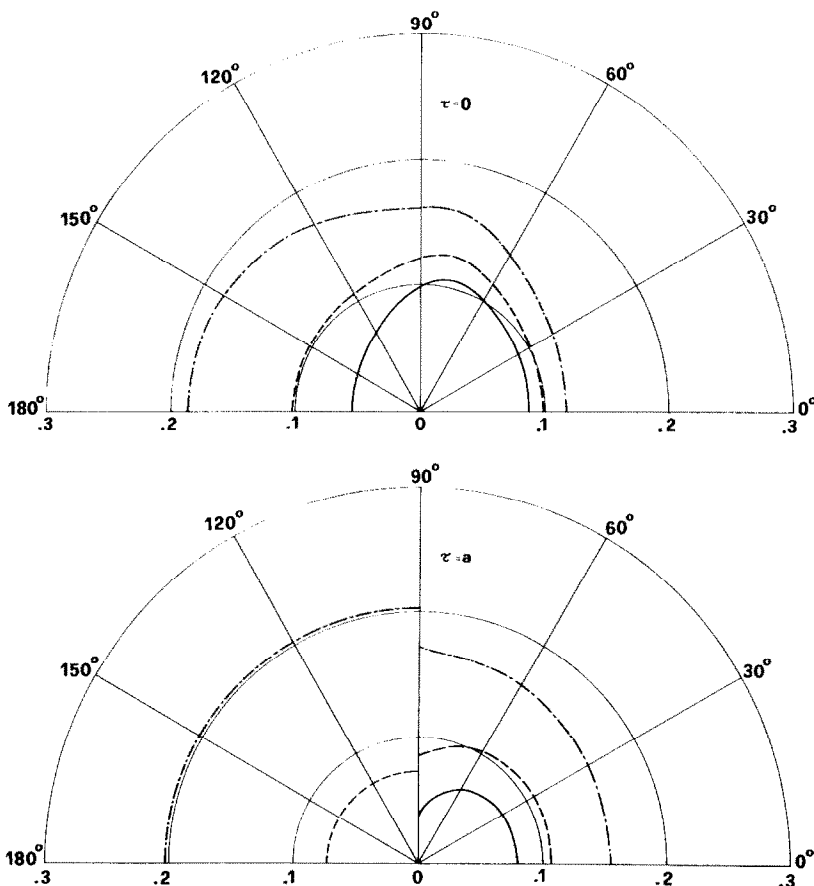


FIG. 8. Rayleigh scattering: the angular distribution of the radiation intensity $I(\tau, \mu)$ for $a = 1$, $c = 0.9$.
 (— $\rho = 0$, - - - $\rho = 0.5$, - · - · - $\rho = 1$).

REFERENCES

1. V. C. Boffi and G. Spiga, Integral theory of radiative heat transfer with anisotropic scattering and general boundary conditions, *J. Math. Phys.* **18**, 2448–2455 (1977).
2. R. O. Buckius and M. M. Tseng, Radiative heat transfer in a planar medium with anisotropic scattering and directional boundaries, *J. Quant. Spectros. Radiat. Transf.* **20**, 385–402 (1978).
3. L. B. Evans, C. M. Chu and S. W. Churchill, The effect of anisotropic scattering on radiant transport, *J. Heat Transfer* **87C**, 381–387 (1965).
4. A. Dayan and C. L. Tien, Heat transfer in a gray planar medium with linear anisotropic scattering, *J. Heat Transfer* **97C**, 391–396 (1975).
5. A. Dayan and C. L. Tien, Radiative transfer with anisotropic scattering in an isothermal slab, *J. Quant. Spectros. Radiat. Transf.* **16**, 113–125 (1976).
6. H. L. Beach, M. N. Ozisik and C. E. Siewert, Radiative transfer in linearly anisotropic-scattering, conservative and non-conservative slabs with reflective boundaries, *Int. J. Heat Mass Transfer* **14**, 1551–1565 (1971).
7. V. C. Boffi, F. Santarelli and C. Stramigioli, Integral transform method in radiative transfer, *J. Quant. Spectros. Radiat. Transf.* **18**, 189–203 (1977).
8. V. C. Boffi, F. Santarelli and C. Stramigioli, Rigorous constructive solutions in radiative heat transfer, *Int. J. Engng Sci.* **15**, 607–621 (1977).
9. L. V. Kantorovich and G. P. Akilov, *Functional Analysis in Normed Spaces*, Pergamon, Oxford (1964).
10. V. C. Boffi, F. Santarelli, G. Spiga and C. Stramigioli, Radiative transfer in an absorbing scattering slab bounded by emitting and reflecting surfaces, *Int. J. Heat Mass Transfer* **22**, 1705–1717 (1979).
11. R. Viskanta and J. S. Toor, Radiant energy transfer in waters, *Water Resources Res.* **8**, 595–608 (1972).
12. R. Viskanta and J. S. Toor, Effect of multiple scattering on radiant energy transfer in waters, *J. Geophys. Res.* **78**, 3538–3551 (1973).
13. M. Abramowitz and I. A. Stegun, *Handbook of Mathematical Functions*, Dover, New York (1970).
14. V. C. Boffi, V. G. Molinari and G. Spiga, Anisotropy of scattering and fission in neutron transport theory, *Nucl. Sci. Engng* **64**, 823–836 (1977).
15. H. Kschwendt, The Fourier transform of a product of two spherical Bessel functions, *Atomkernenergie* **15**, 122–126 (1970).

APPENDIX 1

In equation (8a)

$$\begin{aligned}
 K_{00}(x) &= E_1(x), \\
 K_{01}(x) &= K_{10}(x) = E_2(x), \\
 K_{11}(x) &= E_3(x), \\
 K_{02}(x) &= K_{20}(x) = \frac{3}{2}E_3(x) - \frac{1}{2}E_1(x), \\
 K_{12}(x) &= K_{21}(x) = \frac{3}{2}E_4(x) - \frac{1}{2}E_2(x), \\
 K_{22}(x) &= \frac{9}{2}E_5(x) - \frac{3}{2}E_3(x) + \frac{1}{4}E_1(x).
 \end{aligned}$$

In equation (7b), when $h(\mu) = \delta(\mu - 1)$

$$F_0(x) = \exp(-(a+x)) + 2\rho \exp(-2a)E_2(a-x),$$

$$F_1(x) = \exp(-(a+x)) - 2\rho \exp(-2a)E_3(a-x),$$

$$F_2(x) = \exp(-(a+x)) + \rho \exp(-2a)[3E_4(a-x) - E_2(a-x)].$$

In equation (8b), when $g(\mu) = 2$

$$G_0(x) = 2E_2(a-x),$$

$$G_1(x) = 2E_3(a-x),$$

$$G_2(x) = 3E_4(a-x) - E_2(a-x).$$

In equation (6), when $g(\mu) = 2$

$$H_{00}(\tau, \tau') = E_1(|\tau - \tau'|) + 2\rho E_2(a - \tau)E_2(a - \tau'),$$

$$H_{01}(\tau, \tau') = \operatorname{sgn}(\tau - \tau')E_2(|\tau - \tau'|) + 2\rho E_2(a - \tau)E_3(a - \tau'),$$

$$H_{10}(\tau, \tau') = \operatorname{sgn}(\tau - \tau')E_2(|\tau - \tau'|) - 2\rho E_3(a - \tau)E_2(a - \tau'),$$

$$H_{11}(\tau, \tau') = E_3(|\tau - \tau'|) - 2\rho E_3(a - \tau)E_3(a - \tau'),$$

$$H_{02}(\tau, \tau') = \frac{3}{2}E_3(|\tau - \tau'|) - \frac{1}{2}E_1(|\tau - \tau'|) + \rho E_2(a - \tau)[3E_4(a - \tau') - E_2(a - \tau')],$$

$$H_{20}(\tau, \tau') = \frac{3}{2}E_3(|\tau - \tau'|) - \frac{1}{2}E_1(|\tau - \tau'|) + \rho[3E_4(a - \tau) - E_2(a - \tau)]E_2(a - \tau'),$$

$$H_{22}(\tau, \tau') = \frac{9}{4}E_5(|\tau - \tau'|) - \frac{3}{2}E_3(|\tau - \tau'|) + \frac{1}{4}E_1(|\tau - \tau'|) + \frac{1}{2}\rho[3E_4(a - \tau) - E_2(a - \tau)][3E_4(a - \tau') - E_2(a - \tau')].$$

APPENDIX 2

The integral in equation (17) can be solved by a Taylor series expansion of Legendre polynomials, which yields

$$U_n^s(x) = \sum_{k=0}^n \frac{(2k-1)!!}{a^k k!} C_{n-k}^{[k+(1/2)]} \left(\frac{x}{a}\right) \times [(-1)^k X_k^s(a+x) + (-1)^s X_k^s(a-x)],$$

where $(2k-1)!! = (2k-1)(2k-3)\dots 5.3.1$, C_{n-k} is a Gegenbauer ultraspherical polynomial [13], and

$$X_k^s(x) = \int_0^x y^k E_{1+s}(y) dy.$$

All $X_k^s(x)$ can be evaluated by the recursion formula

$$X_k^s(x) = \frac{1}{k+1} [X^{k+1} E_{1+s}(x) + X_{k+1}^{s-1}],$$

starting from

$$X_k^{-1}(x) = \gamma(k, x)$$

where γ is the well known incomplete gamma function [13]. An analogous technique is successful with the evaluation of equation (18). We get

$$D_n^s = \sum_{k=0}^n \frac{(-1)^k (2k-1)!! (n+k)!}{a^k k! (2k)! (n-k)!} Y_k^{s+2},$$

where

$$Y_k = \int_0^{2a} y^k E_r(y) dy = X_k^{-1}(2a).$$

As regards C_{mn}^s , equation (21), we first rearrange the double integral as

$$C_{mn}^s = a[(-1)^{m+n} + (-1)^s] \int_0^{2a} E_{1+s}(y) \times \int_{-1}^{1-y/a} P_n(x) P_n\left(x + \frac{y}{a}\right) dx dy,$$

and then use Kschwendt's result [15], to put the last integral in the form of a polynomial of degree $m+n+1$ with respect to y . Setting

$$\beta_{\nu}^{mn} = \begin{cases} \frac{2\delta_{mn}}{2m+1} & \nu = 0 \\ -1 & \nu = 1 \\ \frac{2(-1)^\nu}{(\nu-1)!(\nu+1)!} \prod_{k=1}^{\nu-1} (m+n+1+\nu-2k) & \nu = 2, 3, \dots, m+n+1 \end{cases} \times (|m-n| + \nu - 2k)$$

where δ_{mn} is the Kronecker symbol, the result reads as

$$C_{mn}^s = (-1)^{(n-m+|n-m|)/2} [(-1)^{m+n} + (-1)^s] a \times \sum_{\nu=0}^{m+n+1} \frac{\nu+1}{(2a)^\nu \nu!} \beta_{\nu}^{mn} Y_{\nu}^{s+2}.$$

The integral in equation (23) can be handled again by a Taylor expansion of Legendre polynomials, and yields simply

$$E_n = (-1)^n \sum_{k=0}^n \frac{(-1)^k (2k-1)!! (n+k)!}{a^k k! (2k)! (n-k)!} \gamma(k+1, 2a).$$

The same procedure is in order for the functions W_n , equation (25), and G_n^s , equation (27), which are thus expressed as

$$W_n(\tau, \mu) = \sum_{k=0}^n \frac{(-1)^k (2k-1)!!}{a^k k!} \mu^k C_{n-k}^{(k+1/2)} \left(\frac{\tau}{a}\right) \gamma\left(k+1, \frac{a+\tau}{\mu}\right)$$

and

$$G_n^s(\tau) = \sum_{k=0}^n \frac{(-1)^k (2k-1)!!}{a^k k!} C_{n-k}^{(k+1/2)} \left(\frac{\tau}{a}\right) X_k^{1+s}(a+\tau),$$

respectively.

TRANSFERT RADIATIF DANS UNE PLAQUE ABSORBANTE ET ANISOTROPIQUEMENT DIFFUSANTE AVEC UNE FRONTIERE REFLECHISSANTE

Résumé—On considère le transfert radiatif dans une plaque plane en supposant qu'un rayonnement externe frappe normalement une face, tandis que l'autre face réfléchit de façon diffuse. On considère aussi bien les mécanismes de diffusion anisotropiques linéaires et de Rayleigh. Une solution rigoureuse est développée en suivant une procédure basée sur des méthodes projectives: les formules résultantes ont été obtenues numériquement pour obtenir la distribution des variables physiques sensibles, pour quelques situations intéressantes.

STRAHLUNGSWÄRMEÜBERGANG IN EINER ABSORBIERENDEN UND
ANISOTROP STREUENDEN PLATTE MIT EINER REFLEKTIERENDEN
BEGRENZUNG

Zusammenfassung—Es wird der Strahlungswärmeaustausch in einer ebenen Platte untersucht, wobei die von außen aufgeprägte Strahlung senkrecht auf die eine Begrenzung der Platte trifft, während die andere Begrenzung diffus reflektiert. Die Streuerverteilung im linear anisotropen Fall und nach Rayleigh werden beide betrachtet. Es wird eine genaue Lösung entwickelt, die sich an ein Konstruktionsverfahren anlehnt, welches auf Projektionsmethoden beruht. Die daraus gewonnenen Rechenformeln sind numerisch weiterverarbeitet worden, um die Verteilung der physikalisch relevanten Größen für einige wichtige Fälle zu bekommen.

ЛУЧИСТЫЙ ПЕРЕНОС В ПОГЛОЩАЮЩЕЙ И АНИЗОТРОПНО РАССЕЙВАЮЩЕЙ
ПЛИТЕ С ОТРАЖАЮЩЕЙ ПОВЕРХНОСТЬЮ

Аннотация— Исследован лучистый перенос в проницаемой плоской плите в предположении, что поток излучения нормально падает на одну из ее поверхностей и отражается диффузно от другой. Рассмотрены как линейно анизотропная, так и релеевская моды рассеяния. С помощью проекционных методов получено строгое решение. В результате численной обработки расчетных формул определены физические переменные для ряда практически важных случаев.